

Original article

# Titin-mediated thick filament activation stabilizes myofibrils on the descending limb of their force–length relationship

Gudrun Schappacher-Tilp

*Institute of Mathematics and Scientific Computing, University of Graz, Heinrichstraße 36, 8010 Graz, Austria*

Received 31 October 2017; received 17 December 2017; accepted 29 December 2017

Available online 17 May 2018

## Abstract

**Purpose:** The aim of this study was to extend current half-sarcomere models by involving a recently found force-mediated activation of the thick filament and analyze the effect of this mechanosensing regulation on the length stability of half-sarcomeres arranged in series.

**Methods:** We included a super-relaxed state of myosin motors and its force-dependent activation in a conventional cross-bridge model. We simulated active stretches of a sarcomere consisting of 2 non-uniform half-sarcomeres on the descending limb of the force–length relationship.

**Results:** The mechanosensing model predicts that, in a passive sarcomere on the descending limb of the force–length relationship, the longer half-sarcomere has a higher fraction of myosin motors in the on-state than the shorter half-sarcomere. The difference in the number of myosin motors in the on-state ensures that upon calcium-mediated thin filament activation, the force-dependent thick filament activation keeps differences in active force within 20% during an active stretch. In the classical cross-bridge model, the corresponding difference exceeds 80%, leading to great length instabilities.

**Conclusion:** Our simulations suggest that, in contrast to the classical cross-bridge model, the mechanosensing regulation is able to stabilize a system of non-uniform half-sarcomeres arranged in series on the descending limb of the force–length relationship.

© 2018 Published by Elsevier B.V. on behalf of Shanghai University of Sport. This is an open access article under the CC BY-NC-ND license. (<http://creativecommons.org/licenses/by-nc-nd/4.0/>).

**Keywords:** Force–length relationship; Instability; Mathematical modelling; Myofibril; Thick filament activation

## 1. Introduction

Until recently, it was well accepted that the main regulator of active force production after calcium-mediated activation in sarcomeres is the amount of actin–myosin overlap and, therefore, the length of a half-sarcomere.<sup>1–3</sup> When half-sarcomeres are arranged in series in equilibrium, they are supposed to exert exactly the same force; however, it has been consistently reported that half-sarcomeres in myofibrils are highly non-uniform in length.<sup>4,5</sup> With length as the main regulator, non-uniformities in sarcomere length translate to non-uniform regulation of active force production. Therefore, it has been hypothesized that a myofibril, consisting of sarcomeres arranged in series, is inherently unstable.<sup>1,6,7</sup> Under perturbation, due to the negative slope of the force–length curve on the descending limb of the force–length relationship, stronger sarcomeres will shorten or stretch only slightly, whereas weaker sarcomeres will

eventually yield. The yielding sarcomeres are stretched rapidly beyond the actin–myosin overlap until they reach a length where the passive force equals the active force of the stronger sarcomeres.<sup>8,9</sup> This so-called sarcomere popping is supposed to be most prominent under significant perturbations such as active stretches on the descending limb of the force–length relationship.<sup>7,8,10</sup> However, although sarcomeres are clearly non-uniform in length, these non-uniformities do not appear to increase during active stretches,<sup>11,12</sup> and in a number of studies<sup>13–17</sup> popping events have not been observed. Moreover, sarcomeres cover a variety of different lengths rather than being grouped into 2 distinct populations after active stretches.<sup>18</sup> In addition, half-sarcomeres that are longer during an isometric contraction are not necessarily the ones with the greatest elongations during a subsequent active stretch.<sup>13,16</sup> A recent study showed sarcomere popping during active stretches, but sarcomere popping was even more frequently observed under supposedly stable isometric conditions.<sup>12</sup> These results indicate that sarcomere popping might occur if non-uniformities are extreme but is not limited to perturbations of the system.

Peer review under responsibility of Shanghai University of Sport.

E-mail address: [gudrun.schappacher-tilp@uni-graz.at](mailto:gudrun.schappacher-tilp@uni-graz.at)

<https://doi.org/10.1016/j.jshs.2018.05.002>

2095-2546/© 2018 Published by Elsevier B.V. on behalf of Shanghai University of Sport. This is an open access article under the CC BY-NC-ND license.

(<http://creativecommons.org/licenses/by-nc-nd/4.0/>)

To conclude, while sarcomeres arranged in series in a myofibril are clearly non-uniform in length, they seem to be stable and able to produce similar forces at different degrees of actin–myosin overlap. Therefore, it seems highly likely that actin–myosin overlap is not the only active isometric force regulating mechanism.

A candidate for an additional regulating mechanism introducing stability in a myofibril is the recently discovered tension-dependent activation of thick filaments.<sup>19</sup> Electron microscopy studies have shown that a subpopulation of myosin motors is in a “super-relaxed” state bound to each other along the myosin filament core.<sup>20–23</sup> These super-relaxed myosin motors inhibit ATP-ase activity in non-activated muscles.<sup>24</sup> Myosin motors have to transit from the super-relaxed state to an on-state in order to participate in the cross-bridge working cycle. This transition is regulated by different mechanisms in different muscle types. In some invertebrate striated muscles, it is regulated by calcium binding to myosin;<sup>25</sup> in smooth vertebrate muscle cells, it is regulated by the phosphorylation of the myosin regulatory light chain.<sup>26,27</sup> In vertebrate skeletal muscles, it has been proposed that the transition from super-relaxed state to on-state is governed by the mechanical stress in the thick filament.<sup>19</sup> Linari et al.<sup>19</sup> used X-ray diffraction to show that in relaxed muscle fibers at optimal myosin–actin overlap, only a small fraction, around 5%, of myosin motors are in the on-state. These 5% of myosin motors are sufficient for a muscle to react upon calcium activation when the external load is low. At high loads, the increase in active force triggers a positive-feedback loop by enhancing the transition of myosin motors from the super-relaxed state to the on-state. Force increases after calcium-mediated thin filament activation can be approximated by a single exponential curve with a time delay of 18 ms and a time constant of 34 ms. Myosin filaments in the on-state will transit back to the super-relaxed state if filament stress is decreasing. When the fiber is rapidly shortened by 10% fiber length, force recovery follows a single exponential curve with a time constant of 28 ms and a time delay of 10 ms. This result indicates that some, but not all, myosin motors have moved back to the super-relaxed state during the low-load period.

Recently, it was discovered that the transition from the super-relaxed state to the on-state in skinned rabbit fibers is triggered by passive forces as well.<sup>28</sup> Fusi et al.<sup>28</sup> were able to

show that the extension of the giant protein titin triggers the transition of myosin motors from the super-relaxed state to the on-state in passive fibers with a force-dependent rate between 100/s and 500/s. Moreover, based on different activation levels of calcium combined with blebbistatin, which inhibits active force production, the results of this study indicated that the titin-mediated transition is, in fact, calcium independent. Thus, the number of cross bridges in the on-state depends only on filament force regardless of whether that force is generated actively by myosin motors or by the extension of titin.

The role of super-relaxed myosin motors is debated because it has various prominent physiological properties, like the Frank–Starling mechanism of the heart<sup>29–32</sup> (i.e., the increased ejection volume correlates with increased end diastolic volumes in ventricles). Recently, a theoretical study showed that including a super-relaxed state in a classical cross-bridge model<sup>33</sup> provides a solution to a well-known conflict between high power output at intermediate shortening velocities and, therefore, high attachment and detachment rates of myosin motors and the slow rise in force upon calcium-mediated activation of the thin filament.<sup>34</sup>

Here, we hypothesize that titin-mediated thick filament activation regulation could also stabilize the system of non-uniform half-sarcomeres arranged in series. While short half-sarcomeres on the descending limb of the force–length curve have a more favorable actin–myosin overlap than long half-sarcomeres, long half-sarcomeres have higher passive forces and therefore more myosin motors in the on-state than short sarcomeres. Upon calcium-mediated actin activation, the subsequent positive-feedback loop could provide a powerful mechanism to ensure stability of the non-uniform myofibril system (Fig. 1).

The aim of this study was to build a sarcomere model using a force-dependent activation of myosin motors to test the hypothesis that titin-mediated mechanosensing stabilizes the system of non-uniform half-sarcomeres on the descending limb of the force–length relationship.

## 2. Methods

In order to include mechanosensing in a model, we augmented a classical three-state cross-bridge model<sup>35</sup> with a super-relaxed state (Fig. 2).

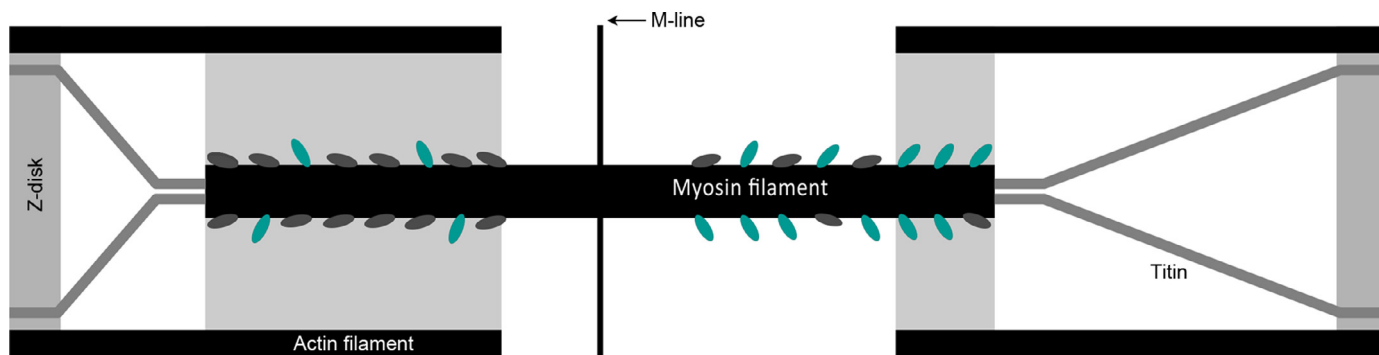


Fig. 1. Sketch of a (non-activated) sarcomere consisting of 2 non-uniform half-sarcomeres. Although actin–myosin overlap of the left half-sarcomere is greater, its fraction of myosin motors in the on-state (green) is smaller due to the smaller extension of titin and therefore smaller passive force compared to the half-sarcomere on the right.

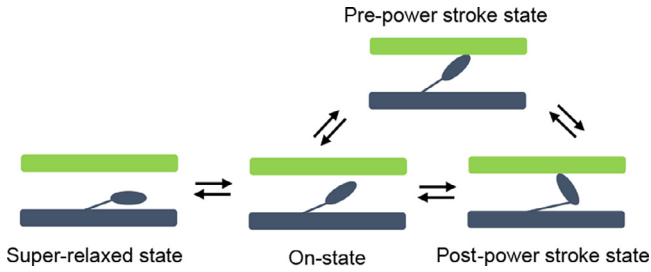


Fig. 2. The classical three-state cross-bridge working cycle augmented by a super-relaxed state.

Each myosin head follows the cycle scheme depicted in Fig. 2. Rate functions of the working cycle (i.e., on-state, pre-power stroke state, and post-power stroke state) are based on the literature.<sup>36</sup> We chose a force-dependent rate function for the transition from the super-relaxed state to the on-state to match experimental data. Specifically, we chose the rate function such that at  $3.6 \mu\text{m}$  with an average force of  $65 \text{ pN}$  per titin filament, 15% of the myosin motors are in the on-state.<sup>28</sup> To simplify the model, we chose a constant backward rate such that in a relaxed muscle below titin's slack length, 5% of myosin motors are in the on-state. To compare the stabilizing properties of the mechanosensing model with the classical cross-bridge model, we ran all simulations based on the classical cross-bridge model comprised of the on-state, the pre-power stroke state, and post-power stroke state. The rates of the working cycle are the same for both models.

Passive forces are predicted by a structural titin model allowing individual immunoglobulin domains to unfold in the presence of high forces.<sup>37</sup> We introduce length non-uniformities by randomly assigning different passive force capacities to the half-sarcomeres. Because calcium-mediated activation of the thin filament is much faster than force development,<sup>38</sup> we do not model a calcium gradient explicitly but assume a quasi-instantaneous thin filament activation.

Finally, we follow the M-line by calculating the active and passive forces in each step of the simulation. Moreover, we calculated the external viscous force, which is assumed to be proportional to the velocity of the M-line (Fig. 3). To simplify the model we assume that internal viscoelasticity is roughly the same for both half-sarcomeres and can therefore be omitted. A detailed model description is presented in Appendix 1.

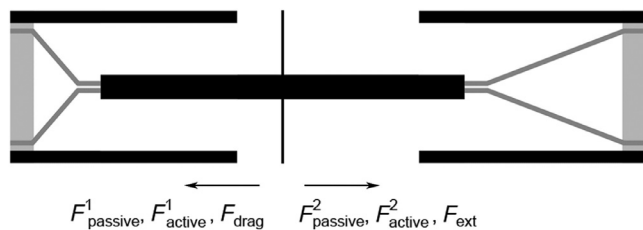


Fig. 3. Sketch of the sarcomere model. The motion of the M-line is governed by active forces ( $F_{\text{active}}^{1,2}$ ), passive forces ( $F_{\text{passive}}^{1,2}$ ), external viscous force ( $F_{\text{drag}}$ ), and external forces ( $F_{\text{ext}}$ ).

### 3. Results

We test the stabilizing properties of the mechanosensing model by passively stretching a non-uniform sarcomere to a sarcomere length of  $3.2 \mu\text{m}$ . We impose an instantaneous calcium-mediated activation of the thin filament, wait for 1 s to reach quasi-steady-state isometric forces, and subsequently stretch the sarcomere for 2 s. To avoid artifacts to jumps in stretching velocity, we simulated a stretch ramp. The velocity was assumed to rise linearly within the first 200 ms from  $0 \mu\text{m/s}$  to  $0.1 \mu\text{m/s}$  and stay constant for the remaining 1800 ms. The difference in passive force between the 2 half-sarcomeres leads to a difference in half-sarcomere lengths of  $0.2 \mu\text{m}$  at  $3.2 \mu\text{m}$  sarcomere length. Upon calcium-mediated thin filament activation, the long half-sarcomere begins to stretch slowly in the classical cross-bridge model. In the mechanosensing model, the long half-sarcomere remains at a stable length for the first 100 ms. During active stretching, both models predict that the long half-sarcomere takes up more of the sarcomere stretching. However, although the mechanosensing model predicts that the shorter half-sarcomere will elongate throughout the stretch, the classical model predicts a shortening of the shorter half-sarcomere toward the end of the stretch, leading to greater non-uniformities (Fig. 4).

In order to compare the active force capacity between half-sarcomeres during stretch, we normalized the difference in active forces between the half-sarcomeres to the force of the short half-sarcomere. The difference in active force in the mechanosensing model stays within 20%; however, the difference in the classical cross-bridge model exceeds 80% at the end of the active stretch (Fig. 5).

We analyzed results of both models for 6 exemplar starting points. Under quasi-isometric conditions (i.e., the sarcomere length is fixed at  $3.2 \mu\text{m}$ ), the classical cross-bridge model predicts shortening of the short half-sarcomere. In the presence of length non-uniformities greater than 250 nm at the time of

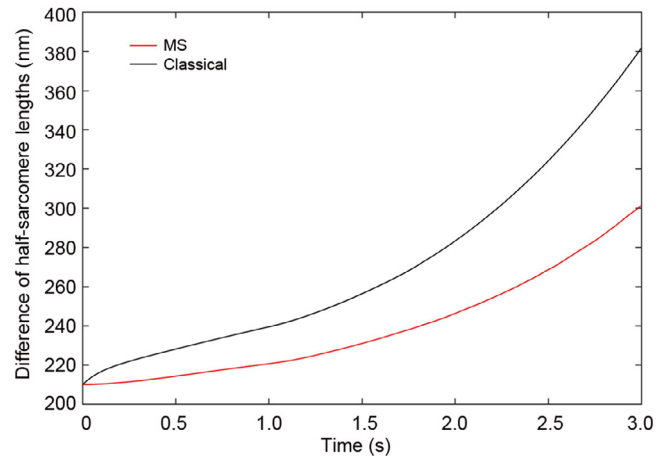


Fig. 4. Differences in half-sarcomere lengths for an isometric contraction (first second) and subsequent stretching (Seconds 1–3). In the mechanosensing model (MS, red line), the long half-sarcomere is stable for the first 100 ms, whereas in the classical model (classical, black line), the long half-sarcomere is immediately being stretched. Although differences in half-sarcomere lengths increase over time, the differences are significantly smaller in the MS than in the classical model.

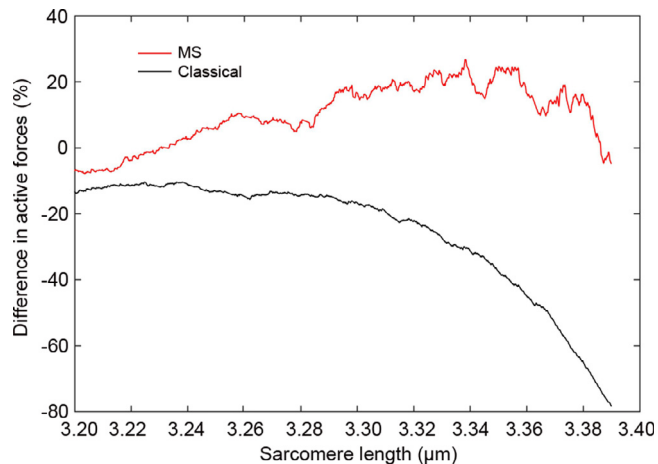


Fig. 5. Differences in the active half-sarcomere forces during sarcomere stretching. Forces are normalized to the forces of the short half-sarcomere. Differences in active half-sarcomere force are significantly smaller in the mechanosensing model (MS, red line) than in the classical cross-bridge model (classical, black line).

calcium-mediated thin filament activation, the classical cross-bridge model predicts shortening of the short half-sarcomere for the active stretch following the isometric contraction. The mechanosensing model predicts almost constant half-sarcomere lengths for the quasi-isometric conditions and lengthening of the short half-sarcomere in the subsequent active stretch (Fig. 6).

4. Discussion

Recent experimental results revealed a force-dependent activation of the thick filament in vertebrate skeletal muscles.<sup>19,21</sup> The relevance of this regulation for physiological

muscle contraction has not been fully assessed experimentally. In this study, we used a mechanosensing mechanism as a stabilizer for a sarcomere consisting of 2 non-uniform half-sarcomeres on the descending limb of the force-length relationship. Although the long half-sarcomere has less actin-myosin overlap, the fraction of myosin motors in the on-state is higher than in the short half-sarcomere. Upon calcium-mediated thin filament activation, this increased fraction of on-state cross bridges triggers a positive-feedback loop recruiting and increasing the number of activated cross-bridges. The proportion of cross bridges able to participate in the working cycle is therefore higher in the long half-sarcomere compared to the short half-sarcomere. If the initial non-uniformity between half-sarcomeres is within limits (i.e., the long half-sarcomere can still produce enough active force to trigger the positive-feedback loop), the sum of the active and passive forces in each half-sarcomere are comparable and prevent the development of dramatic half-sarcomere length non-uniformities. The simulation results are in close agreement with experimental findings, indicating that non-uniform half-sarcomeres are able to exert similar total forces even when perturbed by active stretching of the sarcomere.

Due to the positive-feedback loop between the instantaneous force in the thick filament and the number of cross-bridges in the on-state, simulations are numerically expensive. Therefore, the simulation of a myofibril consisting of hundreds of half-sarcomeres arranged in series is an extreme task that we have not performed yet. However, because the principle of the model is independent of the number of sarcomeres, we anticipate similar stabilizing effects in an entire myofibril simulation.

It is worth noting that the stabilizing effect is associated with non-negligible passive forces. At lengths with negligible

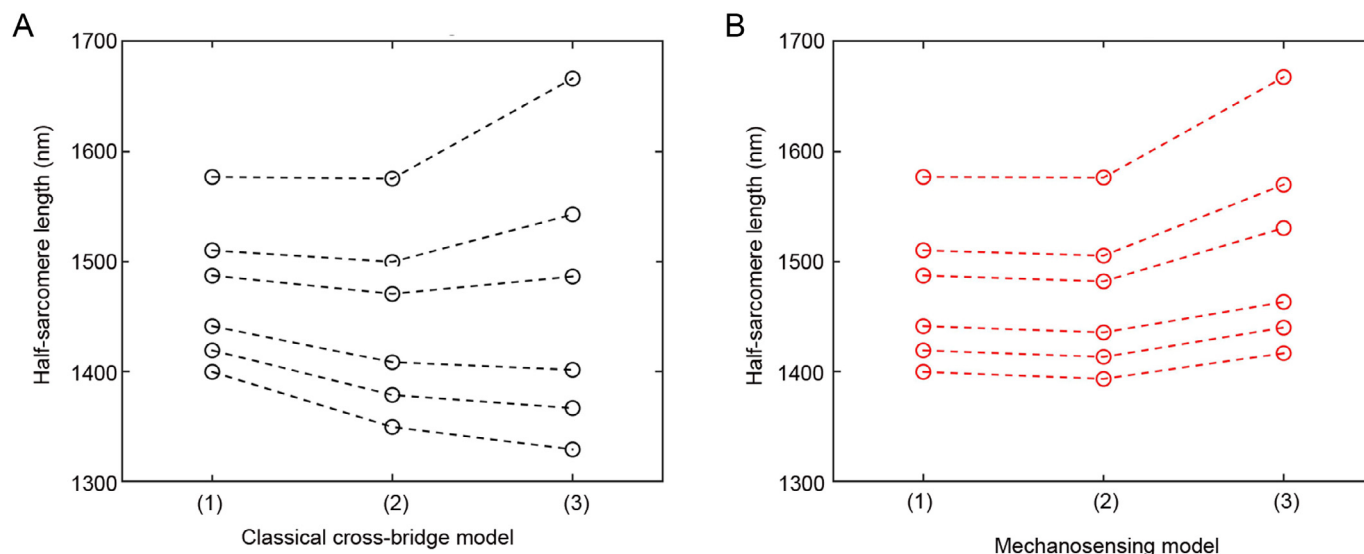


Fig. 6. Half-sarcomere lengths of the short half-sarcomere before calcium-mediated thin filament activation (1), after 1 s of quasi-isometric contraction (2), and after 2 s of active stretching (3) of 25 non-uniform sarcomeres. Although the classical cross-bridge model (A) always predicts shortening during the quasi-isometric contraction, half-sarcomere lengths remain stable in the mechanosensing model. Furthermore, the mechanosensing model (B) predicts lengthening of the half-sarcomeres or all levels of length non-uniformities. This is in contrast to the classical cross-bridge model, which predicts shortening of half-sarcomeres for sarcomeres with half-sarcomere length differences greater than 250 nm before activation.

passive forces, the number of myosin motors in the super-relaxed state is the same for all half-sarcomeres. In cardiac muscle, titin is short and has high stiffness, resulting in high passive forces at physiologically relevant sarcomere lengths.<sup>39–42</sup> Therefore, the regulating mechanism of the mechanosensing model would come into effect at much shorter sarcomere lengths in cardiac muscles than in skeletal muscles.

There are limitations in this study. Filament compliance is not included in the model. Because filament compliance affects force rise and the force–velocity curves,<sup>43–45</sup> it would be interesting to see the effects of filament compliance on the mechanosensing regulation. Moreover, we did not include the recently hypothesized actin–titin binding.<sup>46–48</sup> Because the free length of titin is significantly reduced when bound to the actin filament, we would anticipate higher regulatory effects of the mechanosensing mechanism for conditions when titin is bound to actin.

## 5. Conclusion

Instability on the descending limb of the force–length relationship is a rather counterintuitive hypothesis. A number of human and animal skeletal muscles have been shown to work on the descending limb of the force–length relationship.<sup>49</sup> An inherently unstable system with frequent dramatic sarcomere elongations due to common perturbations, such as active stretches (e.g., in the quadriceps muscles during downstairs walking), does not seem a likely choice for an exquisitely designed and highly efficient motor such as skeletal muscle. The proposed mechanosensing mechanism acts like a safety system. At long lengths, the mechanism senses the need to overcome the disadvantage of an activation at an unfavorable length and recruits a greater fraction of myosin motors from the super-relaxed state. If half-sarcomere lengths differ substantially, the proposed regulating mechanism is not able to prevent sarcomere popping, as the lack of actin–myosin overlap at very long lengths cannot be compensated for by an increased number of cross bridges in the on-state. This observation agrees with experimental results. In studies involving long average sarcomere lengths and great sarcomere length non-uniformities (SD = 0.9  $\mu\text{m}$ ), sarcomere popping has been observed even for isometric conditions.<sup>12</sup> In the presence of small, physiologically relevant half-sarcomere length differences, the proposed mechanism provides an intriguingly simple solution for preventing half-sarcomere and sarcomere length instabilities and associated muscle injury. Perturbations of the transition between super-relaxed cross bridges and on-state cross bridges result in high instabilities.

To conclude, our study indicates for the first time that the mechanosensing model could close a gap between theory and experimental results regarding instabilities during eccentric muscle contractions. It remains to be proven experimentally if the mechanosensing model proposed here is indeed a major component in the stability of half-sarcomeres in a myofibril.

## Competing interests

The author declares that she has no competing interests.

## Appendix 1

Mean field approximation of the cross-bridge cycle:

- $S$  Fraction of cross bridges in the super-relaxed state
- $D$  Fraction of cross bridges in the on-state
- $p_1$  Fraction of cross bridges in the pre-power stroke state
- $p_2$  Fraction of cross bridges in the post-power stroke state

Then, the following system determines the fraction of cross bridges in each state:

$$\frac{dS}{dt} = -k_{\text{on}}(T(t))S + k_{\text{off}}D \quad (\text{A1})$$

$$\begin{aligned} \frac{dD}{dt} = & k_{\text{on}}(T(t))S - \left( k_{\text{off}} + \int_{-\infty}^{\infty} k_{12}(x)dx \right) D \\ & + \int_{-\infty}^{\infty} (k_{21}(x)p_1(x, t) + k_{31}(x)p_2(x, t)) dx \end{aligned} \quad (\text{A2})$$

$$\begin{aligned} \frac{\partial p_1}{\partial t} + v(t) \frac{\partial p_1}{\partial t} = & \left( \int_{-\infty}^{\infty} k_{12}(x)dx \right) D - (k_{21}(x) + k_{23}(x))p_1(x, t) \\ & + k_{32}(x + x_{\text{ps}})p_2(x + x_{\text{ps}}, t) \end{aligned} \quad (\text{A3})$$

$$\begin{aligned} \frac{\partial p_2}{\partial t} + v(t) \frac{\partial p_2}{\partial t} = & k_{23}(x - x_{\text{ps}})p_1(x - x_{\text{ps}}, t) - (k_{32}(x) + k_{31}(x))p_2(x, t) \end{aligned} \quad (\text{A4})$$

$$S(t) + D(t) + \int_{-\infty}^{\infty} (p_1(x, t) + p_2(x, t)) dx \equiv 1 \quad (\text{A5})$$

where  $x_{\text{ps}}$  is the length change in the cross-bridge link associated with the power stroke.

For the classical cross-bridge model equation, we used the same set of equations but set  $S \equiv 0$ ,  $k_{\text{on}} \equiv 0$ ,  $k_{\text{off}} \equiv 0$ , thereby reducing the model to the traditional three-state cross-bridge model.

Active force as a function of time and half-sarcomere length  $hsl$  is calculated as

$$F_a(t) = N_{\text{heads}} \cdot \text{Geometry}(hsl) \cdot \int_{-\infty}^{\infty} k_{\text{xb}} \cdot x \cdot (p_1(x, t) + p_2(x, t)) dx \quad (\text{A6})$$

The velocity  $v(t)$  is dependent on the movement of the M-line and is different for each half-sarcomere. The geometry function is based on Minozzo et al.<sup>50</sup> classical cross-bridge

rate functions adapted from Campbell.<sup>36</sup>  $T$  is the sum of active and passive force normalized to the number of thick filaments in a half-sarcomere and measured in pN. We assume that in a myofibril of rabbit psoas with a diameter of 1  $\mu\text{m}$  the number of myosin heads ( $N_{\text{heads}}$ ) is  $90 \cdot 10^3$  and that there are roughly 320 thick filaments per half-sarcomere.<sup>51</sup>

### Passive forces

The simulations are based on the 3.400-kD isoform of rabbit psoas<sup>52</sup> consisting of 50 proximal immunoglobulin domains, 26 distal immunoglobulin domains forming end-filaments, and 800 PEVK residues.<sup>53</sup> A detailed mathematical formulation is given in Schappacher-Tilp et al.<sup>37</sup>

### Sarcomere model

We simplify the sarcomere model by assuming that internal friction force in both half-sarcomeres is approximately the same. The viscous drag coefficient was set to 6.5  $\text{nN} \cdot \text{s}/\mu\text{m}$ .<sup>54</sup> The model was implemented in MATLAB routines.

### References

- Hill AV. The mechanics of active muscle. *Proc R Soc Lond B Biol Sci* 1953;**141**:104–17.
- Huxley AF, Niedergerke R. Structural changes in muscle during contraction: interference microscopy of living muscle fibres. *Nature* 1954;**173**: 971–3.
- Gordon AM, Huxley AF, Julian FJ. The variation in isometric tension with sarcomere length in vertebrate muscle fibres. *J Physiol* 1966;**184**:170–92.
- Julian FJ, Morgan DL. Intersarcomere dynamics during fixed-end tetanic contractions of frog-muscle fibers. *J Physiol* 1979;**293**:365–78.
- Edman KA, Reggiani C. Redistribution of sarcomere-length during isometric contraction of frog-muscle fibers and its relation to tension creep. *J Physiol* 1984;**351**:169–98.
- Morgan DL. New insights into the behavior of muscle during active lengthening. *Biophys J* 1990;**57**:209–21.
- Morgan DL. An explanation for residual increased tension in striated muscle after stretch during contraction. *Exp Physiol* 1994;**79**:831–8.
- Allinger TL, Epstein M, Herzog W. Stability of muscle fibers on the descending limb of the force-length relation. A theoretical consideration. *J Biomech* 1996;**29**:627–33.
- Walcott S, Herzog W. Modeling residual force enhancement with generic cross-bridge models. *Math Biosci* 2008;**216**:172–86.
- Zahalak GI. Can muscle fibers be stable on the descending limbs of their sarcomere length-tension relations. *J Biomech* 1997;**30**:1179–82.
- Edman KA, Elzinga G, Noble MI. Residual force enhancement after stretch of contracting frog single muscle fibers. *J Gen Physiol* 1982;**80**: 769–84.
- Johnston K, Jinha A, Herzog W. The role of sarcomere length non-uniformities in residual force enhancement of skeletal muscle myofibrils. *R Soc Open Sci* 2016;**3**:150657. doi:10.1098/rsos.150657.
- Telley IA, Stehle R, Ranatunga KW, Pfitzer G, Stüssi E, Denoth J. Dynamic behaviour of half-sarcomeres during and after stretch in activated rabbit psoas myofibrils: sarcomere asymmetry but no “sarcomere popping”. *J Physiol* 2006;**573**:173–85.
- Rassier DE, Herzog W, Pollack GH. Dynamics of individual sarcomeres during and after stretch in activated single myofibrils. *Proc Biol Sci* 2003;**270**:1735–40.
- Joumaa V, Leonard TR, Herzog W. Residual force enhancement in myofibrils and sarcomeres. *Proc Biol Sci* 2008;**275**:1411–9.
- Pavlov I, Novinger R, Rassier DE. Sarcomere dynamics in skeletal muscle myofibrils during isometric contractions. *J Biomech* 2009;**42**: 2808–12.
- Pun C, Syed A, Rassier DE. History-dependent properties of skeletal muscle myofibrils contracting along the ascending limb of the force–length relationship. *Proc Biol Sci* 2010;**277**:475–84.
- Herzog W, Powers K, Johnston K, Duvall M. A new paradigm for muscle contraction. *Front Physiol* 2015;**6**:174. doi:10.3389/fphys.2015.00174.
- Linari M, Brunello E, Reconditi M, Fusi L, Caremani M, Narayanan T, et al. Force generation by skeletal muscle is controlled by mechanosensing in myosin filaments. *Nature* 2015;**528**:276–9.
- Woodhead JL, Zhao FQ, Craig R, Egelman EH, Alamo L, Padrón R. Atomic model of a myosin filament in the relaxed state. *Nature* 2005;**436**:1195–9.
- Fusi L, Huang Z, Irving M. The conformation of myosin heads in relaxed skeletal muscle: implications for myosin-based regulation. *Biophys J* 2015;**109**:783–92.
- Reconditi M, Brunello E, Linari M, Bianco P, Narayanan T, Panine P, et al. Motion of myosin head domains during activation and force development in skeletal muscle. *Proc Natl Acad Sci USA* 2011;**108**:7236–40.
- Alamo L, Wriggers W, Pinto A, Bartoli F, Salazar L, Zhao F, et al. Three-dimensional reconstruction of tarantula myosin filaments suggests how phosphorylation may regulate myosin activity. *J Mol Biol* 2008;**384**:780–97.
- Stewart MA, Franks-Skiba K, Chen S, Cooke R. Myosin ATP turnover rate is a mechanism involved in thermogenesis in resting skeletal muscle fibers. *Proc Natl Acad Sci USA* 2010;**107**:430–5.
- Woodhead JL, Zhao FQ, Craig R. Structural basis of the relaxed state of a  $\text{Ca}^{2+}$ -regulated myosin filament and its evolutionary implications. *Proc Natl Acad Sci USA* 2013;**110**:8561–6.
- Wendt T, Taylor D, Trybus KM, Taylor K. Three-dimensional image reconstruction of dephosphorylated smooth muscle heavy meromyosin reveals asymmetry in the interaction between myosin heads and placement of subfragment 2. *Proc Natl Acad Sci USA* 2001;**98**:4361–6.
- Somlyo AV, Khromov AS, Webb MR, Ferenczi MA, Trentham DR, He ZH, et al. Smooth muscle myosin: regulation and properties. *Philos Trans R Soc Lond B Biol Sci* 2004;**359**:1921–30.
- Fusi L, Brunello E, Yan Z, Irving M. Thick filament mechano-sensing is a calcium-independent regulatory mechanism in skeletal muscle. *Nat Commun* 2016;**7**:13281. doi:10.1038/ncomms13281.
- Hooijman P, Stewart MA, Cooke R. A new state of cardiac myosin with very slow ATP turnover: a potential cardioprotective mechanism in the heart. *Biophys J* 2011;**100**:1969–76.
- McNamara JW, Li A, Dos Remedios CG, Cooke R. The role of super-relaxed myosin in skeletal and cardiac muscle. *Biophys Rev* 2015;**7**:5–14.
- Marcucci L, Washio T, Yanagida T. Titin-mediated thick filament activation, through a mechanosensing mechanism, introduces sarcomere-length dependencies in mathematical models of rat trabecula and whole ventricle. *Sci Rep* 2017;**7**:5546. doi:10.1038/s41598-017-05999-2.
- Ait-Mou Y, Hsu K, Farman GP, Kumar M, Greaser ML, Irving TC, et al. Titin strain contributes to the Frank–Starling law of the heart by structural rearrangements of both thin- and thick-filament proteins. *Proc Natl Acad Sci USA* 2016;**113**:2306–11.
- Huxley AF. Muscle structure and theories of contraction. *Prog Biophys Biophys Chem* 1957;**7**:255–318.
- Marcucci L, Reggiani C. Mechanosensing in myosin filament solves a 60 years old conflict in skeletal muscle modeling between high power output and slow rise in tension. *Front Physiol* 2016;**7**:427. doi:10.3389/fphys.2016.00427.
- Duke TA. Molecular model of muscle contraction. *Proc Natl Acad Sci USA* 1999;**96**:2770–5.
- Campbell KS. Interactions between connected half-sarcomeres produce emergent mechanical behavior in a mathematical model of muscle. *PLoS Comput Biol* 2009;**5**:e1000560. doi:10.1371/journal.pcbi.1000560.
- Schappacher-Tilp G, Leonard T, Desch G, Herzog W. Computing average passive forces in sarcomeres in length-ramp simulations. *PLoS Comput Biol* 2016;**12**:e1004904. doi:10.1371/journal.pcbi.1004904.
- Fusi L, Brunello E, Sevrieva IR, Sun YB, Irving M. Structural dynamics of troponin during activation of skeletal muscle. *Proc Natl Acad Sci USA* 2014;**111**:4626–31.
- Granzier HL, Labeit S. The giant protein titin: a major player in myocardial mechanics, signaling, and disease. *Circ Res* 2004;**94**:284–95.

40. LeWinter MM, Granzier H. Cardiac titin: a multifunctional giant. *Circulation* 2010;**121**:2137–45.
41. Watanabe K, Nair P, Labeit D, Kellermayer MS, Greaser M, Labeit S, et al. Molecular mechanics of cardiac titin's PEVK and N2B spring elements. *J Biol Chem* 2002;**277**:11549–58.
42. Linke WA, Fernandez JM. Cardiac titin: molecular basis of elasticity and cellular contribution to elastic and viscous stiffness components in myocardium. *J Muscle Res Cell Motil* 2002;**23**:483–97.
43. Martyn DA, Chase PB, Regnier M, Gordon AM. A simple model with myofilament compliance predicts activation-dependent crossbridge kinetics in skinned skeletal fibers. *Biophys J* 2002;**83**:3425–34.
44. Campbell KS. Filament compliance effects can explain tension overshoots during force development. *Biophys J* 2006;**91**:4102–9.
45. Tanner BC, Daniel TL, Regnier M. Filament compliance influences cooperative activation of thin filaments and the dynamics of force production in skeletal muscle. *PLoS Comput Biol* 2012;**8**:e1002506. doi:10.1371/journal.pcbi.1002506.
46. Herzog W, Duvall M, Leonard TR. Molecular mechanisms of muscle force regulation: a role for titin. *Exerc Sport Sci Rev* 2012;**40**:50–7.
47. Schappacher-Tilp G, Leonard T, Desch G, Herzog W. A novel three-filament model of force generation in eccentric contraction of skeletal muscles. *PLoS One* 2015;**10**:e0141188. doi:10.1371/journal.pone.0117634.
48. Herzog W, Schappacher G, DuVall M, Leonard TR, Herzog JA. Residual force enhancement following eccentric contractions: a new mechanism involving titin. *Physiology (Bethesda)* 2016;**31**:300–12.
49. Burkholder TJ, Lieber RL. Sarcomere length operating range of vertebrate muscles during movement. *J Exp Biol* 2001;**204**:1529–36.
50. Minozzo FC, Baroni BM, Correa JA, Vaz MA, Rassier DE. Force produced after stretch in sarcomeres and half-sarcomeres isolated from skeletal muscles. *Sci Rep* 2013;**3**:2320. doi: 10.1038/srep02320.
51. Linari M, Caremani M, Piperio C, Brandt P, Lombardi V. Stiffness and fraction of myosin motors responsible for active force in permeabilized muscle fibers from rabbit psoas. *Biophys J* 2007;**92**:2476–90.
52. Freiburg A, Trombitas K, Hell W, Cazorla O, Fougères F, Centner T, et al. Series of exon-skipping events in the elastic spring region of titin as the structural basis for myofibrillar elastic diversity. *Circ Res* 2000;**86**:1114–21.
53. Prado LG, Makarenko I, Andresen C, Krüger M, Opitz CA, Linke WA. Isoform diversity of giant proteins in relation to passive and active contractile properties of rabbit skeletal muscles. *J Gen Physiol* 2005;**126**:461–80.
54. Chapin LM, Edgar LT, Blankman E, Beckerle MC, Shiu YT. Mathematical modeling of the dynamic mechanical behavior of neighboring sarcomeres in actin stress fibers. *Cell Mol Bioeng* 2014;**7**:73–85.